Int. J. Solids Structures Vol. 22, No. 8, pp. 859–881, 1986
Printed in Great Britain.

0020-7683/86 $3.00 + .00
Pergamon Journals Ltd.

DYNAMIC PLASTIC DEFORMATION OF AN INFINITE PLATE

CARL K. YOUNGDAHL
Components Technology Division, Argonne National Laboratory, Argonne, IL 60439, U.S.A.

and

DUSAN KRAJCINOVIC
Department of Civil Engineering, Mechanics and Metallurgy, University of Illinois at Chicago, Chicago, IL 60680, U.S.A.

(*Received* 26 *March* 1985; *in revised form* 13 *August* 1985)

Abstract—A solution is derived for the dynamic plastic response of an infinite plate subjected to a general axisymmetric pressure pulse which varies both with position and time and is applied to a time-varying area of the plate. An approximation formula is obtained for the final plastic deformation in terms of simple integrals of the loading.

1. INTRODUCTION

In various structural applications in the nuclear reactor and other industries, design must be based not only on normal operating loads but must also consider unusual transient overloadings which may plastically deform the structure. Details of the spatial and temporal distributions of these unusual loadings are not known in advance, so that analyses and experimental simulations do not duplicate the actual loading conditions and may lead to designs which are either unconservative or, at the other extreme, excessively conservative.

Although finite-element and finite-difference techniques can be used to obtain solutions for specific problems in dynamic plastic deformation, they are often prohibitively expensive to use for parameter studies, and important qualitative features of the results may be lost in the abundance of numerical output. Moreover, the computational precision necessary to numerically obtain convergent and stable solutions to these nonlinear problems requires the specification of the loading and the material properties in much greater detail than that in which they can be realistically predicted. Consequently, there is a need for the development of approximation and bounding methods for dynamic plastic deformation of structures.

Approximation and bounding methods have two important functions. First, they can be used to perform design and safety analyses of structural components, and, in particular, to perform parameter studies over a wide range of design variables and loadings. Second, they can be used to validate computer programs which predict dynamic plastic deformation by strictly numerical methods. Because of the basic nonlinearity of the plastic response, these programs are difficult to validate without having a variety of sample problems to check against.

Much of the development of approximation methods[1–5] has emphasized impact loadings or impulse loadings resulting from explosives attached to the structure. These loadings are very short compared to the duration of the structural response, and the simplifying assumption is made that the impulse is applied over zero time and imparts a uniform initial velocity to the structure. However, in many applications the loading is transmitted to the structure through a fluid, which slows the initial loading rate and spreads the duration of the loading over a time period comparable to the structural response time. Details of the load history and spatial distribution then significantly affect the final plastic deformation.

Two correlation parameters, the impulse and an effective load, were proposed[6] to eliminate the effect of pulse shape on the final plastic deformation of some common structural configurations. For each of these problems, the curves showing the final plastic deformation produced by a wide variety of pulse shapes are essentially collapsed to a single curve if the impulse and effective load are used as correlation parameters. Since these two parameters depend only on integrals of the loading, they are insensitive to perturbations in pulse shape, which is encouraging because details of pulse shapes are difficult to experimentally reproduce and measure. The loading in each case studied in [6] has a fixed spatial shape and is applied to a fixed region of the body, but the magnitude of the loading is a general function of time. In each case, the material is assumed to be rigid, perfectly plastic, which is a common assumption in both static limit-load analysis and the development of bounding methods for dynamic problems. A derivation of the two correlation parameters from energy principles is presented in [7].

The problem treated in this paper is an infinite plate loaded by an axisymmetric dynamic pressure which is an arbitrary function of position and time and which is applied to a growing circular region of the plate. The material of the plate is assumed to be rigid, perfectly plastic. A closed-form solution is obtained which is valid for a wide variety of loadings. An approximate solution for the final plastic deformation of the plate is then proposed in terms of three integral parameters of the loading. If the loading is specialized to a product of position and time (which implies a fixed region of application), these integral parameters reduce to combinations of the two correlation parameters proposed previously.

Several comprehensive review articles on dynamic plasticity are available[8–15], so that an extensive bibliography will not be given here. Some papers which are particularly relevant to the problem discussed here are [16, 17], which treat a finite circular plate acted on by a uniform dynamic pressure with various pulse shapes, and [18–21], which consider the uniform pressure to be applied only to a central region. Reference [22] considers an infinite plate loaded uniformly over a circular region and develops an approximate method of solution for arbitrary pulse shape.

2. STATEMENT OF PROBLEM

Consider an infinite plate subjected to a dynamic pressure $P(r, t)$, where r is the radial coordinate and t is time, applied over a time-dependent circular region having radius $R(t)$. Under the usual assumptions of small deflection theory of thin plates, the equations of motion are

$$\frac{\partial^2(rM_r)}{\partial r^2} - \frac{\partial M_\theta}{\partial r} = \mu r\frac{\partial V}{\partial t} - rP, \tag{2.1}$$

$$V = \partial W/\partial t, \tag{2.2}$$

where $M_r(r, t)$ and $M_\theta(r, t)$ are the radial bending moment and circumferential bending moment per unit arc length, respectively, μ is the mass per unit surface area, and $V(r, t)$ and $W(r, t)$ are the lateral velocity and deflection. Let the radial and circumferential rates of curvature be denoted by κ_r and κ_θ, respectively. Then

$$\begin{aligned} \kappa_r &= -\partial^2 V/\partial r^2, \\ \kappa_\theta &= -(1/r)(\partial V/\partial r). \end{aligned} \tag{2.3}$$

The material of the plate is assumed to be rigid, perfectly plastic, and insensitive to strain-rate. The limited interaction yield condition of Fig. 1 will be used here. The three plastic regimes which occur in the plate are point A, segment AB, and point B of Fig. 1. From the yield condition and flow rule, the restrictions on the bending moments and rates of curvature for these regimes are

$$\text{Regime } A: \quad M_r = -M_0, \quad M_\theta = M_0, \quad \kappa_r \leqslant 0, \quad \kappa_\theta \geqslant 0. \tag{2.4}$$

$$\text{Regime } AB: \quad -M_0 < M_r < M_0, \quad M_\theta = M_0, \quad \kappa_r = 0, \quad \kappa_\theta \geqslant 0. \tag{2.5}$$

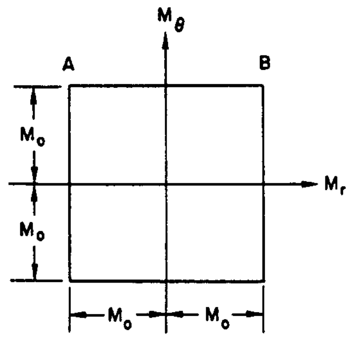

Fig. 1. Yield condition.

$$\text{Regime } B: \quad M_r = M_0, \quad M_\theta = M_0, \quad \kappa_r \geqslant 0, \quad \kappa_\theta \geqslant 0. \tag{2.6}$$

Therefore,

$$M_\theta = M_0 \tag{2.7}$$

at every point in the plate where plastic deformation occurs.

The basic deformation mode has a hinge at $r = 0$ and a moving hinge circle at $r = \rho(t)$. The central hinge is in Regime B, the moving hinge in Regime A, and the region in between is in Regime AB. The corresponding boundary conditions and restrictions are, at $r = 0$,

$$M_r = M_0, \quad \partial M_r/\partial r = 0, \quad \partial^2 M_r/\partial r^2 < 0, \tag{2.8}$$

while at $r = \rho(t)$,

$$M_r = -M_0, \quad \partial M_r/\partial r = 0, \quad \partial^2 M_r/\partial r^2 > 0, \quad V = 0. \tag{2.9}$$

For $0 < r < \rho(t)$,

$$-M_0 < M_r < M_0, \quad \partial^2 V/\partial r^2 = 0, \quad \partial V/\partial r \leqslant 0. \tag{2.10}$$

The conditions on M_r given by eqns (2.9) and (2.10) assure that a maximum occurs at $r = 0$ and a minimum at $r = \rho$. If $\partial^2 M_r/\partial r^2 = 0$ at the moving hinge at some time during the motion, a hinge band in Regime A begins to form there. Correspondingly, if $\partial^2 M_r/\partial r^2 = 0$ at $r = 0$, a hinge band in Regime B will then begin to form in a region about the center of the plate. The conditions on a moving hinge band are

$$M_r = -M_0, \quad \partial^2 V/\partial r^2 \geqslant 0, \quad \partial V/\partial r \geqslant 0, \tag{2.11}$$

for $\rho_1(t) \leqslant r \leqslant \rho_2(t)$. For a central hinge band,

$$M_r = M_0, \quad \partial^2 V/\partial r^2 \leqslant 0, \quad \partial V/\partial r \leqslant 0, \tag{2.12}$$

for $0 \leqslant r \leqslant \rho_0(t)$.

The plate is at rest until time t_y when the yield load is first reached; the initial conditions are thus

$$V(r, t_y) = W(r, t_y) = 0. \tag{2.13}$$

3. SOLUTION FOR BASIC DEFORMATION MODE

Guided by the solution for the finite plate and eqns (2.9) and (2.10), the basic velocity mode having a central hinge and a moving hinge circle is taken as

$$V(r,t) = V_0(t)\left[\frac{\rho(t)-r}{\rho(t)}\right], \tag{3.1}$$

where V_0 is the velocity at the plate center. Substitution into eqn (2.1) and integration with respect to r then gives, using eqns (2.7) and (2.8),

$$M_r(r,t) = M_0 + \frac{r^2}{12}\left[2-\frac{r}{\rho(t)}\right]\mu\dot{V}_0(t) + \frac{r^3}{12\rho^2(t)}\mu V_0(t)\dot{\rho}(t) - \int_0^r \bar{r}P(\bar{r},t)\,\mathrm{d}\bar{r} + \frac{1}{r}\int_0^r \bar{r}^2P(\bar{r},t)\,\mathrm{d}\bar{r}, \tag{3.2}$$

where the dots denote differentiation with respect to time. The boundary conditions from eqn (2.9) then imply

$$\begin{aligned}\rho^2\dot{V}+\rho V_0\dot{\rho} &= -\frac{24M_0}{\mu}+\frac{12}{\mu}\int_0^\rho rP(r,t)\,\mathrm{d}r-\frac{12}{\mu\rho}\int_0^\rho r^2P(r,t)\,\mathrm{d}r,\\ \rho\dot{V}_0+3V_0\dot{\rho} &= \frac{12}{\mu\rho^2}\int_0^\rho r^2P(r,t)\,\mathrm{d}r.\end{aligned} \tag{3.3}$$

Algebraic manipulation of eqns (3.3) gives

$$\begin{aligned}\frac{\mathrm{d}}{\mathrm{d}t}(\rho^2V_0) &= \frac{6}{\mu}\left[\int_0^\rho rP(r,t)\,\mathrm{d}r-2M_0\right],\\ \frac{\mathrm{d}}{\mathrm{d}t}(\rho^3V_0) &= \frac{12}{\mu}\int_0^\rho r^2P(r,t)\,\mathrm{d}r.\end{aligned} \tag{3.4}$$

The solution to eqn (3.4) is, using the initial conditions (2.13),

$$\begin{aligned}\rho(t) &= \frac{2\displaystyle\int_{t_y}^t\int_0^{\rho(\bar{t})} r^2P(r,\bar{t})\,\mathrm{d}r\,\mathrm{d}\bar{t}}{\displaystyle\int_{t_y}^t\int_0^{\rho(\bar{t})} rP(r,\bar{t})\,\mathrm{d}r\,\mathrm{d}\bar{t}-2M_0(t-t_y)},\\ V_0(t) &= \frac{3\left[\displaystyle\int_{t_y}^t\int_0^{\rho(\bar{t})} r^2P(r,\bar{t})\,\mathrm{d}r\,\mathrm{d}\bar{t}-2M_0(t-t_y)\right]^3}{2\mu\left[\displaystyle\int_{t_y}^t\int_0^{\rho(\bar{t})} r^2P(r,\bar{t})\,\mathrm{d}r\,\mathrm{d}\bar{t}\right]^2}.\end{aligned} \tag{3.5}$$

Substitution back into eqn (3.2) gives the radial bending moment distribution for $0 \leqslant r \leqslant \rho(t)$,

$$\begin{aligned}M_r(r,t) = {}&\left(1-\frac{6r^2}{\rho^2}+\frac{4r^3}{\rho^3}\right)M_0-\int_0^r \bar{r}P(\bar{r},t)\,\mathrm{d}\bar{r}\\ &+\frac{1}{r}\int_0^r \bar{r}^2P(\bar{r},t)\,\mathrm{d}\bar{r}+\left(\frac{3r^2}{\rho^2}-\frac{2r^3}{\rho^3}\right)\int_0^\rho rP(r,t)\,\mathrm{d}r\\ &+\left(\frac{3r^3}{\rho^4}-\frac{4r^2}{\rho^3}\right)\int_0^\rho r^2P(r,t)\,\mathrm{d}r.\end{aligned} \tag{3.6}$$

Let L_1 and L_2 be defined by

$$L_1 = \frac{\partial^2 M_r}{\partial r^2} \quad \text{at} \quad r = 0,$$
$$L_2 = \frac{\partial^2 M_r}{\partial r^2} \quad \text{at} \quad r = \rho(t). \tag{3.7}$$

Then

$$L_1(t) = \frac{6}{\rho^2}\int_0^\rho rP(r,t)\,\mathrm{d}r - \frac{8}{\rho^3}\int_0^\rho r^2P(r,t)\,\mathrm{d}r - \frac{12}{\rho^2}M_0 - \frac{1}{3}P(0,t) < 0,$$
$$L_2(t) = -\frac{6}{\rho^2}\int_0^\rho rP(r,t)\,\mathrm{d}r + \frac{12}{\rho^3}\int_0^\rho r^2P(r,t)\,\mathrm{d}r + \frac{12}{\rho^2}M_0 - P(\rho,t) > 0. \tag{3.8}$$

By eqns (2.8) and (2.9), a hinge band will form at the center of the plate if L_1 becomes positive, and an outer hinge band will form if L_2 becomes negative.

The first of eqns (3.5) is an implicit expression for the hinge circle radius since $\rho(t)$ appears as an upper limit in the integrals. If $P(r, t)$ has a long "tail" as r increases, then $\rho(t)$ may be less than $R(t)$, and an iterative solution is needed; only a few steps are needed for convergence because the values of the integrals are only weakly dependent on ρ for this type of pressure distribution. For most of the pressure distributions considered in this investigation, the hinge circle is outside the region of load application for the entire duration of the response. Equation (3.5) then gives an explicit expression for ρ since $R(t)$ replaces $\rho(t)$ as the limit of integration.

Define F, G, I_F, I_G and F_y by

$$F(t) = \int_0^{R(t)} rP(r,t)\,\mathrm{d}r,$$
$$G(t) = \int_0^{R(t)} r^2P(r,t)\,\mathrm{d}r,$$
$$I_F(t) = \int_{t_y}^{t} F(\bar{t})\,\mathrm{d}\bar{t}, \tag{3.9}$$
$$I_G(t) = \int_{t_y}^{t} G(\bar{t})\,\mathrm{d}\bar{t},$$
$$F_y = 2M_0.$$

The quantity $F(t)$ is the time-dependent force applied to a unit sector of the plate, and $G(t)$ is the moment of the pressure about the origin; I_F and I_G are the corresponding impulses associated with F and G; and F_y is the force required to initiate yielding of the plate. For the case when $\rho(t) > R(t)$ for all t, eqns (3.5) and (3.8) become

$$\rho(t) = \frac{2I_G(t)}{I_F(t) - (t-t_y)F_y}, \tag{3.10}$$

$$V_0(t) = \frac{3[I_F(t) - (t-t_y)F_y]^3}{2\mu I_G^2(t)}, \tag{3.11}$$

$$L_1(t) = \frac{6}{\rho^2}[F(t) - F_y] - \frac{8}{\rho^3}G(t) - \frac{1}{3}P(0,t), \tag{3.12}$$

$$L_2(t) = -\frac{6}{\rho^2}[F(t)-F_y] + \frac{12}{\rho^3}G(t). \tag{3.13}$$

It is readily shown that L_2 is proportional to $\dot{\rho}$ for $\rho > R$. Consequently, an outer hinge band does not form if ρ is an increasing function of time, but a band will begin to form if the hinge circle starts to move inward. In general, ρ tends to increase if the applied force F decreases, and vice versa. As a result, if the force is instantaneously applied and then decays, no outer hinge band appears, but a more gradually applied force produces a hinge band.

The occurrence of a central hinge band depends strongly on the shape of the pressure distribution on the plate. A central band usually does not occur if P decreases with r, which is the most realistic situation. Consequently, the formulation for a central band will not be pursued further.

The motion stops at time t_f when V_0 becomes zero. By eqn (3.11), t_f is found from

$$(t_f - t_y)F_y = I_F(t_f) = \int_{t_y}^{t_f} F(t)\,dt. \tag{3.14}$$

Therefore, the average force applied to the plate during the deformation is the yield force F_y.

4. SOLUTION FOR OUTER HINGE BAND

Consider an outer hinge band which begins to form at time t_b, i.e. $L_2(t_b) = 0$. The hinge circle at $\rho(t_b) = \rho_b$ spreads into a band between $\rho_1(t)$ and $\rho_2(t)$ where conditions (2.11) apply. We will assume that the hinge band lies outside the region of load application since this simplifies the solution considerably and is the most usual case. The plate velocity at ρ_1 will be denoted by $V_1(t)$, and the plate velocity at ρ_2 is zero, so that

$$V(\rho_1(t), t) = V_1(t), \tag{4.1}$$

$$V(\rho_2(t), t) = 0, \tag{4.2}$$

$$V_1(t_b) = 0, \tag{4.3}$$

$$\rho_1(t_b) = \rho_2(t_b) = \rho(t_b) = \rho_b. \tag{4.4}$$

In the region $\rho_1 \leqslant r \leqslant \rho_2$, $M_r = -M_0$ and $M_\theta = M_0$. The differential equation (2.1) is then equivalent to

$$\mu\frac{\partial V}{\partial t} = P(r, t) = 0, \tag{4.5}$$

since $r \geqslant \rho_1(t) > R(t)$ by assumption. Therefore,

$$V(r, t) = V_b(r) \qquad \text{for} \qquad \rho_1 \leqslant r \leqslant \rho_2 \tag{4.6}$$

where the function V_b is determined by the remainder of the solution. By eqn (4.2),

$$V_b(\rho_2) = 0 \tag{4.7}$$

which implies that ρ_2 remains fixed, i.e.

$$\rho_2(t) = \rho_b, \tag{4.8}$$

while eqn (4.1) gives

$$V_b(\rho_1) = V_1(t). \tag{4.9}$$

As ρ_1 moves inwards it generates values of $V_b(r)$ until it reaches its minimum position ρ_{1m} at some time t_m. It moves back outward then until it reaches its original location at some time t_c such that

$$\rho_1(t_c) = \rho_b. \tag{4.10}$$

The hinge band now disappears and is replaced with a hinge circle $\rho(t)$.

In the region $0 \leqslant r \leqslant \rho_1(t)$, we take

$$V(r,t) = \frac{V_0(t)[\rho_1(t)-r]+rV_1(t)}{\rho_1(t)}, \tag{4.11}$$

which satisfies eqns (2.10) and matches the hinge band solution at $r = \rho_1$. For convenience, define $f(t)$ by

$$f(t) = \frac{V_0(t)-V_1(t)}{\rho_1(t)}. \tag{4.12}$$

The substitution of eqns (4.11) and (4.12) into eqn (2.1), integration with respect to r, and the application of the boundary conditions $M_r = M_0$ at $r = 0$ and $M_r = -M_0$, $\partial M_r/\partial r = 0$ at $r = \rho_1$ results in two equations in $\dot{V}_0$ and $\dot{f}$; these become, after some algebraic manipulation,

$$\mu\dot{V}_0 = \frac{18}{\rho_1^2}[F(t)-F_y] - \frac{24}{\rho_1^3}G(t), \tag{4.13}$$

$$\mu\dot{f} = \frac{24}{\rho_1^3}[F(t)-F_y] - \frac{36}{\rho_1^4}G(t). \tag{4.14}$$

The bending moment distribution is given by

$$\begin{aligned} M_r(r,t) = {} & \left(1 - \frac{6r^2}{\rho_1^2} + \frac{4r^3}{\rho_1^3}\right)M_0 + \left(\frac{3r^2}{\rho_1^2} - \frac{2r^3}{\rho_1^3}\right)F(t) \\ & + \left(\frac{3r^3}{\rho_1^4} - \frac{4r^2}{\rho_1^3}\right)G(t) - \int_0^r \bar{r}P(\bar{r},t)\,\mathrm{d}\bar{r} \\ & + \frac{1}{r}\int_0^r \bar{r}^2P(\bar{r},t)\,\mathrm{d}\bar{r}. \end{aligned} \tag{4.15}$$

It can be shown (see analogous derivation in [17]) that $\partial^2 M_r/\partial r^2 = 0$ at $r = \rho_1$ during the interval $t_b \leqslant t \leqslant t_m$ when ρ_1 is moving inward. Setting the second derivative of eqn (4.15) equal to zero at ρ_1 results in an equation which can be solved for ρ_1 to give

$$\rho_1(t) = \frac{2G(t)}{F(t)-F_y}, \qquad t_b \leqslant t \leqslant t_m. \tag{4.16}$$

Equations (4.13) and (4.14) can then be integrated to give, using eqn (4.12),

$$V_0(t) = \frac{3}{2\mu}\int_{t_b}^{t} \frac{[F(\bar{t})-F_y]^3}{G^2(\bar{t})}\,\mathrm{d}\bar{t} + V_0(t_b), \tag{4.17}$$

$$V_1(t) = -\frac{3}{4}\rho_1(t)\int_{t_b}^{t}\frac{[F(\bar{t})-F_y]^4}{G^3(\bar{t})}\,d\bar{t} + V_0(t) - \frac{\rho_1(t)}{\rho_b}V_0(t_b). \tag{4.18}$$

Let

$$t = T(\rho_1), \qquad \rho_{1m} \leqslant \rho_1 \leqslant \rho_b, \qquad t_b \leqslant t \leqslant t_m, \tag{4.19}$$

be the inverse relation to eqn (4.16). Then $T(r)$ is the time when ρ_1 moved through position r while traveling inward. Equations (4.9) and (4.17)–(4.19) yield

$$V_b(r) = \frac{3}{2\mu}\int_{t_b}^{T(r)}\frac{[F(t)-F_y]^3}{G^2(t)}\,dt - \frac{3r}{4\mu}\int_{t_b}^{T(r)}\frac{[F(t)-F_y]^4}{G^3(t)}\,dt + \left(1-\frac{r}{\rho_b}\right)V_0(t_b). \tag{4.20}$$

This completes the solution for the interval $t_b \leqslant t \leqslant t_m$. The locations of the inner and outer edges of the band are found from eqns (4.16) and (4.8), V_0 and V_1 are computed from eqns (4.17) and (4.18), and eqns (4.6), (4.20) and (4.11) give the velocity distributions within the band and between the plate center and ρ_1.

In the interval $t_m \leqslant t \leqslant t_c$, the inner edge of the hinge band moves outward until it again reaches its original position ρ_b. Equations (4.1)–(4.15) continue to hold, but now $\partial^2 M_r/\partial r^2 > 0$ and eqn (4.16) for ρ_1 is no longer valid. Since ρ_1 moves back through previous positions, $V_b(r)$ is known for every location that ρ_1 occupies during the interval $t_m \leqslant t \leqslant t_c$ and the plate velocity $V(r, t)$ is known from eqn (4.6) for every point in the hinge band. Letting $r = \rho_1$ in eqn (4.20), we have from eqn (4.9) that

$$V_1(t) = V_b(\rho_1) = \frac{3}{2\mu}\int_{t_b}^{T(\rho_1)}\frac{[F(t)-F_y]^3}{G^2(t)}\,dt - \frac{3\rho_1}{4\mu}\int_{t_b}^{T(\rho_1)}\frac{[F(t)-F_y]^4}{G^3(t)}\,dt + \left(1-\frac{\rho_1}{\rho_b}\right)V_0(t_b). \tag{4.21}$$

Using the definition of $f(t)$ given by eqn (4.12), we can rewrite eqn (4.14) as

$$\dot{V}_0 - \frac{\dot{\rho}_1}{\rho_1}V_0 = \dot{\rho}_1\frac{dV_b}{d\rho_1} - \frac{\dot{\rho}_1}{\rho_1}V_b + \frac{24}{\mu\rho_1^2}[F(t)-F_y] - \frac{36}{\mu\rho_1^3}G(t). \tag{4.22}$$

Equations (4.13) and (4.22) are then equivalent to

$$\rho_1^2\dot{V}_0 + 2\rho_1\dot{\rho}_1V_0 = 2\rho_1\dot{\rho}_1\left(V_b - \rho_1\frac{dV_b}{d\rho_1}\right) + \frac{6}{\mu}[F(t)-F_y], \tag{4.23}$$

$$\rho_1^3\dot{V}_0 + 3\rho_1^2\dot{\rho}_1V_0 = 3\rho_1^2\dot{\rho}_1\left(V_b - \frac{dV_b}{d\rho_1}\right) + \frac{12}{\mu}G(t). \tag{4.24}$$

From eqn (4.21),

$$V_b - \rho_1\frac{dV_b}{d\rho_1} = \frac{3}{2\mu}\int_{t_b}^{T(\rho_1)}\frac{[F(t)-F_y]^3}{G^2(t)}\,dt - \frac{3\rho_1}{2\mu}\frac{[F(T)-F_y]^3}{G^2(T)}\frac{dT}{d\rho_1} + \frac{3\rho_1^2}{4\mu}\frac{[F(T)-F_y]^4}{G^3(T)}\frac{dT}{d\rho_1} + V_0(t_b). \tag{4.25}$$

By eqns (4.16), (4.17) and (4.19), for $t_b \leqslant T \leqslant t_m$,

$$\rho_1(T) = \frac{2G(T)}{F(T)-F_y}, \tag{4.26}$$

$$V_0(T) = \frac{3}{2\mu}\int_{t_b}^{T(\rho_1)} \frac{[F(t)-F_y]^3}{G^2(t)}\,\mathrm{d}t + V_0(t_b). \tag{4.27}$$

Since, by definition of T,

$$\rho_1(t) = \rho_1(T), \qquad t_m \leqslant t \leqslant t_c, \qquad t_b \leqslant T \leqslant t_m, \tag{4.28}$$

eqn (4.25) then becomes

$$V_b - \rho_1 \frac{\mathrm{d}V_b}{\mathrm{d}\rho_1} = V_0(T). \tag{4.29}$$

Noting that

$$\begin{aligned}
&\frac{\mathrm{d}}{\mathrm{d}t}[\rho_1^2 V_0(T)] = 2\rho_1\dot{\rho}_1 V_0(T) + \frac{6}{\rho}[F(T)-F_y]\frac{\mathrm{d}T}{\mathrm{d}\rho_1}\dot{\rho}_1,\\
&\frac{\mathrm{d}}{\mathrm{d}t}[\rho_1^3 V_0(T)] = 3\rho_1^2\dot{\rho}_1 V_0(T) + \frac{12}{\mu}G(T)\frac{\mathrm{d}T}{\mathrm{d}\rho_1}\dot{\rho}_1,\\
&\frac{\mathrm{d}}{\mathrm{d}t}\left[\int_{T(\rho_1)}^{t}[F(\bar{t})-F_y]\,\mathrm{d}\bar{t}\right] = F(t)-F_y-[F(T)-F_y]\frac{\mathrm{d}T}{\mathrm{d}\rho_1}\dot{\rho}_1,\\
&\frac{\mathrm{d}}{\mathrm{d}t}\left[\int_{T(\rho_1)}^{t}G(\bar{t})\,\mathrm{d}\bar{t}\right] = G(t)-G(T)\frac{\mathrm{d}T}{\mathrm{d}\rho_1}\dot{\rho}_1,
\end{aligned} \tag{4.30}$$

we can integrate eqns (4.23) and (4.24) to give

$$\rho_1^2 V_0(t) = \rho_1^2 V_0(T) + \frac{6}{\mu}\int_{T(\rho_1)}^{t}[F(\bar{t})-F_y]\,\mathrm{d}\bar{t} + C_1, \tag{4.31}$$

$$\rho_1^3 V_0(t) = \rho_1^3 V_0(T) + \frac{12}{\mu}\int_{T(\rho_1)}^{t}G(\bar{t})\,\mathrm{d}\bar{t} + C_2. \tag{4.32}$$

The integration constants C_1 and C_2 are both zero because $T = t_m$ when $t = t_m$. Equations (4.31) and (4.32) can be combined to give finally, using eqns (3.9),

$$\rho_1(t) = \frac{2[I_G(t)-I_G(T)]}{I_F(t)-I_F(T)-(t-T)F_y}, \tag{4.33}$$

$$V_0(t) = V_0(T) + \frac{3[I_F(t)-I_F(T)-(t-T)F_y]^3}{2\mu[I_G(t)-I_G(T)]^2}, \tag{4.34}$$

for $t_m \leqslant t \leqslant t_c$. Equation (4.33) is an implicit equation for ρ_1 through eqns (4.19) and (4.26).

At $t = t_c$, ρ_1 returns to its original location ρ_b; since $T(\rho_b) = t_b$, we have from eqn (4.33) that t_c satisfies

$$\rho_b = \frac{2[I_G(t_c)-I_G(t_b)]}{I_F(t_c)-I_F(t_b)-(t_c-t_b)F_y}. \tag{4.35}$$

After t_c, the solution given by eqns (3.10) and (3.11) for the basic deformation mode applies until the motion stops at t_f.

5. EXAMPLES

Examples of three categories of pulses will be presented here: pure impulse, loadings which can be expressed as a product of a function of position and a function of time and pulses applied over a time-varying region.

A. *Pure impulse*

The total force impulse I_{Ff} and moment impulse I_{Gf} are, from eqns (3.9),

$$I_{Ff} = \int_{t_y}^{t_f} \int_0^{R(t)} rP(r, t)\, \mathrm{d}r\, \mathrm{d}t,$$
$$I_{Gf} = \int_{t_y}^{t_f} \int_0^{R(t)} r^2 P(r, t)\, \mathrm{d}r\, \mathrm{d}t. \tag{5.1}$$

The loading on the plate will be called a "pure impulse" if these impulses are applied instantaneously at $t = 0$.

Let V^* be the initial central velocity for a pure impulse. Equations (3.10) and (3.11) then give

$$V^* = 3I_{Ff}^3/2\mu I_{Gf}^2,$$
$$\rho(t) = 2I_{Gf}/(I_{Ff} - F_y t),$$
$$V_0(t) = V^*[(I_{Ff} - F_y t)/I_{Ff}]^3,$$
$$W_0(t) = W^*\{1 - [(I_{Ff} - F_y t)/I_{Ff}]^4\}, \tag{5.2}$$

where

$$W^* = (3/8\mu F_y)(I_{Ff}^4/I_{Gf}^3). \tag{5.3}$$

Since $F_y t_f = I_{Ff}$ by eqn (3.18), $W_0(t_f) = W^*$. Consequently, W^* is the final plastic deformation at the center of the plate produced by a pure impulse characterized by I_{Ff}, I_{Gf}.

B. *Separable loading*

The region of load application must be fixed for loadings which are expressible as the product of functions of position and time. We will take

$$R(t) = R_0,$$
$$P(r, t) = P_0\phi(r)\psi(t), \qquad 0 \leqslant r \leqslant R_0,$$
$$= 0, \qquad r > R_0, \tag{5.4}$$

with $\phi(0) = \psi(0) = 1$ so that P_0 is the initial pressure at the center of the plate. The function ϕ will be called the load shape and the function ψ will be called the pulse shape. Equations (3.9) become

$$F(t) = P_0\psi(t) \int_0^{R_0} r\phi(r)\, \mathrm{d}r,$$
$$G(t) = P_0\psi(t) \int_0^{R_0} r^2\phi(r)\, \mathrm{d}r,$$
$$I_F(t) = P_0 \int_{t_y}^{t} \psi(\bar{t})\, \mathrm{d}\bar{t} \int_0^{R_0} r\phi(r)\, \mathrm{d}r,$$
$$I_G(t) = P_0 \int_{t_y}^{t} \psi(\bar{t})\, \mathrm{d}\bar{t} \int_0^{R_0} r^2\phi(r)\, \mathrm{d}r. \tag{5.5}$$

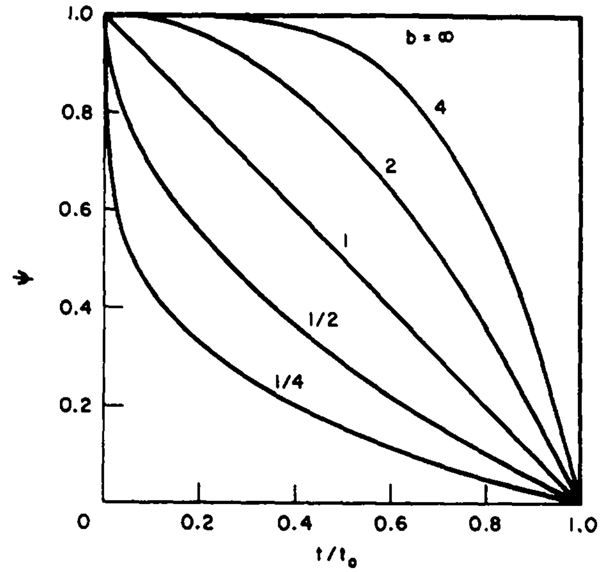

Fig. 2. Pulse shapes.

For concreteness, take

$$\begin{aligned}\phi(r) &= 1-(r/R_0)^a, \qquad 0 \leqslant r \leqslant R_0,\\ \psi(t) &= 1-(t/t_0)^b, \qquad 0 \leqslant t \leqslant t_0,\\ &= 0, \qquad t > t_0,\end{aligned} \tag{5.6}$$

for $a > 0$ and $b > 0$. Figure 2 shows $\psi(t)$ for various values of b. Letting $a \to \infty$ results in a uniform pressure distribution over the load region, and letting $b \to \infty$ results in a rectangular pulse shape in time. Define F_0 as the initial force on the plate; then

$$F_0 = aP_0R_0^2/2(a+2). \tag{5.7}$$

The form of the solution depends on the ratio F_0/F_y. If $F_0/F_y < (b+1)/b$, the deformation stops before t_0. Substitution into eqns (3.10), (3.11) and (3.14) gives, with $\tau = t/t_0$,

$$\begin{aligned}t_f &= t_0[(b+1)(1-F_y/F_0)]^{1/b},\\ \rho(t) &= \frac{4(a+2)F_0R_0(b+1-\tau^b)}{3(a+3)[F_0(b+1-\tau^b)-F_y(b+1)]},\\ V_0(t) &= \frac{27(a+3)^2[F_0(b+1-\tau^b)-F_y(b+1)]^3t}{8(a+2)^2(b+1)\mu F_0^2R_0^2(b+1-\tau^b)^2},\end{aligned} \tag{5.8}$$

$$W_0(t) = \frac{27(a+3)^2F_0t^2}{16(a+2)^2\mu R_0^2}$$

$$\times\left[1-\frac{2\tau^b}{(b+1)(b+2)}-3\frac{F_y}{F_0}+3\left(\frac{F_y}{F_0}\right)^2Q_1(b,\tau)-\left(\frac{F_y}{F_0}\right)^3Q_2(b,\tau)\right],$$

$$0 \leqslant t \leqslant t_f \leqslant t_0,$$

where

$$Q_1(b,\tau) = \frac{2(b+1)}{\tau^2}\int_0^\tau \frac{\bar{\tau}\,d\bar{\tau}}{b+1-\bar{\tau}^b}, \tag{5.9}$$

$$Q_2(b,\tau) = \frac{2(b+1)^2}{t^2}\int_0^\tau \frac{\bar{\tau}\,d\bar{\tau}}{(b+1-\bar{\tau}^b)^2}.$$

For $F_0/F_y \geqslant (b+1)/b$, the equations above for ρ_1, V_0 and W_0 hold for $0 \leqslant t \leqslant t_0$; in the interval $t_0 \leqslant t \leqslant t_f$, the solution is given by

$$t_f = \frac{b}{b+1}\frac{F_0 t_0}{F_y},$$

$$\rho(t) = \frac{4(a+2)bF_0R_0t_0}{3(a+3)[bF_0t_0-(b+1)F_yt]},$$

$$V_0(t) = \frac{27(a+3)^2[bF_0t_0-(b+1)F_yt]^3}{8(a+2)^2b^2(b+1)\mu F_0^2R_0^2t_0^2}, \tag{5.10}$$

$$W_0(t) = W_0(t_0) + \frac{27(a+3)^2(b+1)^2F_0^2t_0^2}{32(a+2)^2b^2\mu R_0^2F_y}\left[\left(\frac{b}{b+1}-\frac{F_y}{F_0}\right)^4-\left(\frac{b}{b+1}-\frac{F_yt}{F_0t_0}\right)^4\right].$$

The final plastic deformation at the center of the loaded region is then, for $F_0/F_y < (b+1)/b$

$$W_0(t_f) = W^*\left[\frac{2b}{b+2}\frac{F_0}{F_y} - \frac{2(3b+4)}{b+2} + \frac{6F_y}{F_0}Q_1\left(b,\frac{t_f}{t_0}\right) - \frac{2F_y^2}{F_0^2}Q_2\left(b,\frac{t_f}{t_0}\right)\right] \tag{5.11}$$

with

$$W^* = \frac{3}{8\mu F_y}\frac{I_{Ff}^4}{I_{Gf}^2} = \frac{27(a+3)^2F_yt_f^2}{32(a+2)^2\mu R_0^2}, \tag{5.12}$$

and for $F_0/F_y \geqslant (b+1)/b$,

$$W_0(t_f) = W^*\left\{1 - \frac{2(b+1)^2}{b(b+2)}\frac{F_y}{F_0} + \left[\frac{6(b+1)^2}{b^2}Q_1(b,1) - \frac{4(b+1)^3}{b^3}\right]\left(\frac{F_y}{F_0}\right)^3 + \left[\frac{(b+1)^4}{b^4} - \frac{2(b+1)^2}{b^2}Q_2(b,1)\right]\left(\frac{F_y}{F_0}\right)^4\right\}, \tag{5.13}$$

with

$$W^* = \frac{3}{8\mu F_y}\frac{I_{Ff}^4}{I_{Gf}^2} = \frac{27(a+3)^2b^2F_0^2t_0^2}{32(a+2)^2(b+1)^2\mu R_0^2F_y}. \tag{5.14}$$

The quantity W^* is again the plastic deformation which would be produced if I_{Ff} and I_{Gf} were applied instantaneously.

The integrals for Q_1 and Q_2 can be readily expressed in closed form for b a small integer or the reciprocal of a small integer; the integrations are easily done numerically for other cases.

For a rectangular pulse ($b \to \infty$), $Q_1 = Q_2 = 1$, and eqn (5.13) simplifies to

$$W_0(t_f) = W^*(1-F_y/F_0)^3(1+F_y/F_0) \tag{5.15}$$

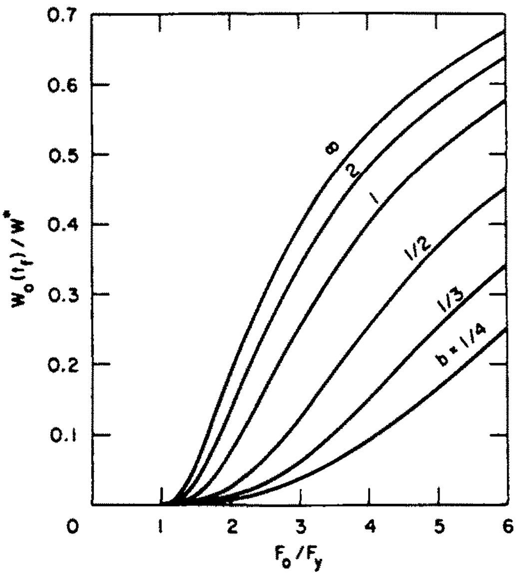

Fig. 3. Final plastic deformation as function of initial force for separable loading example.

with

$$W^* = 27(a+3)^2 F_0^2 t_0^2 / 32(a+2)^2 \mu R_0^2 F_y.$$

Figure 3 shows $W_0(t_f)/W^*$ as a function of F_0/F_y for various values of b; it is not necessary to specify the load shape $\phi(r)$ because its entire effect is included in W^*. Since W^* characterizes the magnitude of the loading, the spread between the curves can be attributed to differences in pulse shape.

In obtaining the solution for the loading given by eqns (5.6), we have assumed that $\rho(t) \geqslant R_0$ and that neither a central hinge band or outer hinge band is formed. From eqns (5.8) and (5.10), $\rho(t) \geqslant R_0$ if

$$F_y/F_0 > (1-a)/3(a+3). \tag{5.16}$$

No central hinge band forms if $L_1(t) < 0$; using eqn (3.12), this is equivalent to

$$\frac{F_y}{F_0} > 1 - \frac{2(a+2)}{3(a+3)}\left[\frac{2(a+3)}{a}\right]^{1/3}. \tag{5.17}$$

No outer hinge band forms if $L_2 > 0$; from eqn (3.13), this is equivalent to

$$\frac{6F_y b}{\rho^2(b+1-t^b/t_0^b)} > 0, \qquad t \leqslant t_0, \tag{5.18}$$

which holds for all positive b. Figure 4 shows the inequalities (5.16) and (5.17) and defines the region for which the above solution is valid.

C. *Varying load region*

Consider loadings of the form

$$\begin{aligned} P(r,t) &= P_0\psi(t)\phi(r/R(t)), \qquad 0 \leqslant r \leqslant R(t), \\ &= 0, \qquad r > R(t), \end{aligned} \tag{5.19}$$

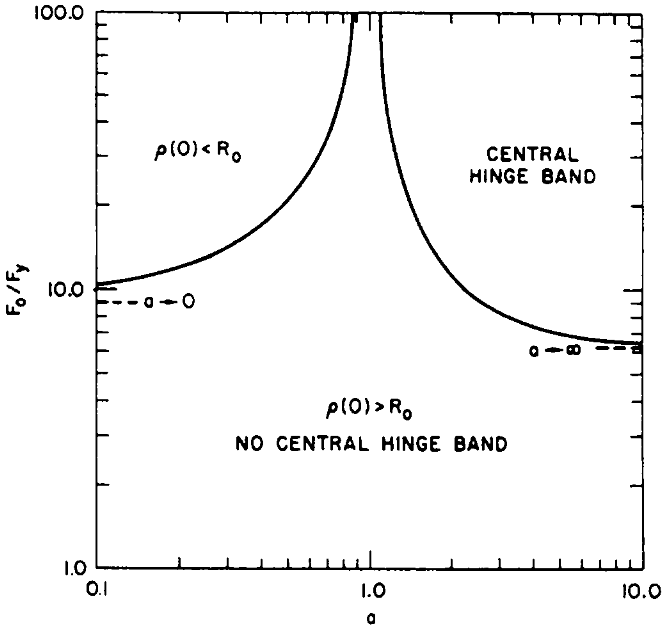

Fig. 4. Region of applicability of solution for separable loading example as function of load shape parameter a.

with

$$R(0) = R_0, \qquad \psi(0) = 1, \qquad \phi(0) = 1. \tag{5.20}$$

To illustrate solutions with hinge bands, let

$$R(t) = R_0(1+t/t_0)^c, \qquad \phi = 1-r/R(t), \tag{5.21}$$

and let $\psi(t)$ be such that the force on the plate increases linearly from F_0 to $2F_0$ in time t_0 and then decreases linearly to zero at time $3t_0$, i.e.

$$\begin{aligned} F(t) &= F_0(1+t/t_0), \qquad 0 \leqslant t \leqslant t_0, \\ &= F_0(3-t/t_0), \qquad t_0 \leqslant t \leqslant 3t_0, \\ &= 0, \qquad t > 3t_0. \end{aligned} \tag{5.22}$$

Consequently,

$$\begin{aligned} P_0 &= 6F_0/R_0^2, \\ \psi(t) &= (1+t/t_0)^{1-2c}, \qquad 0 \leqslant t \leqslant t_0, \\ &= (3-t/t_0)(1+t/t_0)^{-2c}, \qquad t_0 \leqslant t \leqslant 3t_0, \\ &= 0, \qquad t > 3t_0. \end{aligned} \tag{5.23}$$

Results will be shown for the three cases $c = 0$, $\frac{1}{2}$ and 1; these correspond to a fixed load region, a region with a linearly varying area, and a region with a linearly varying radius, respectively. Figure 5 shows $\psi(t)$ for each case. Since $F(t)$ initially increases, an outer hinge band begins to form at $t = 0$, grows in size until t_m, and then decreases until it disappears at t_c. Figure 6 shows the band edge locations $\rho_1(t)$ and $\rho_2(t) = \rho_b$ and the subsequent hinge motion $\rho(t)$ for $F_0 = 1.25F_y$ and $c = 0$, $\frac{1}{2}$ and 1. The plate velocities $V_0(t)$ at the center of the loaded region and inner edge of the hinge band are shown in Figs. 7 and 8, respectively, and the central deformation $W_0(t)$ is given in Fig. 9. Although all three loadings have the

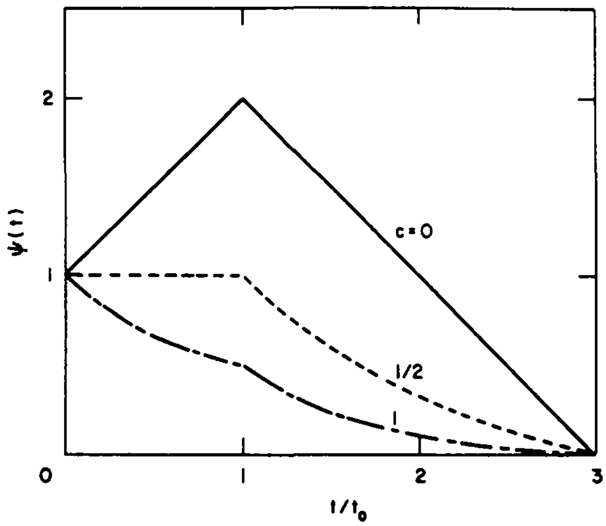

Fig. 5. Pulse shapes for hinge band examples.

same force history $F(t)$ and associated impulse history $I_F(t)$, the responses differ significantly in amplitude because the applied pressure is spread over larger areas as c is increased.

6. CORRELATION OF RESULTS

The solutions to the problems discussed in Refs. [6, 17] for time varying loadings with a fixed spatial distribution were shown to be closely approximated by functions of the impulse and an effective pressure. The effective pressure was defined as the impulse divided by twice the mean time of the pulse, with the mean time being the interval between the onset of plastic deformation and the centroid of the pulse. For a pulse $P(t)$, the impulse I,

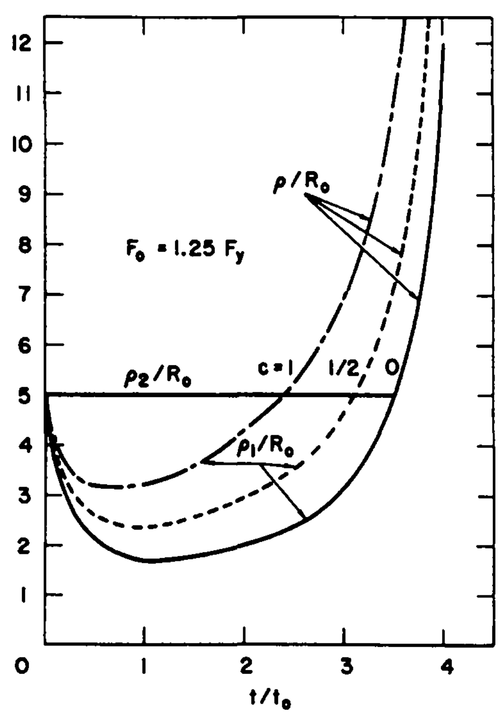

Fig. 6. Hinge band histories.

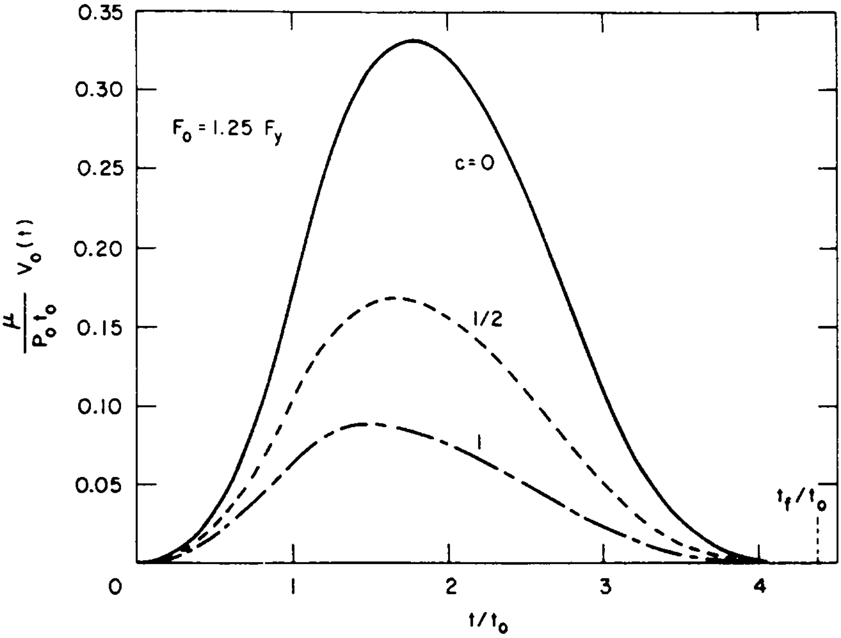

Fig. 7. Velocity history at $r = 0$ for hinge band examples.

mean time t_{mn} and effective pressure P_e are

$$I = \int_{t_y}^{t_f} P(t)\,\mathrm{d}t,$$

$$t_{mn} = \frac{1}{I}\int_{t_y}^{t_f} (t-t_y)P(t)\,\mathrm{d}t, \tag{6.1}$$

$$P_e = I/2t_{mn}.$$

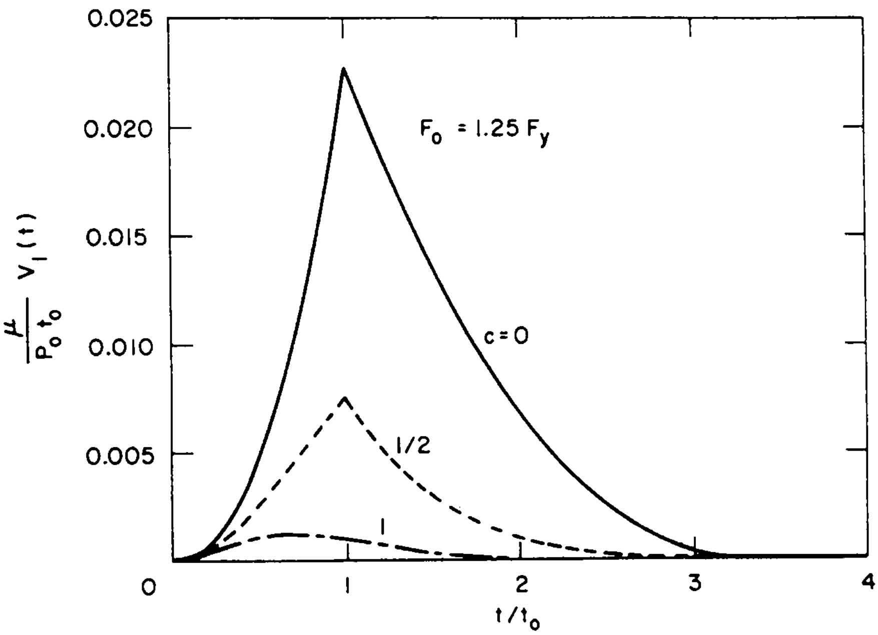

Fig. 8. Velocity history at $r = \rho_1$ for hinge band examples.

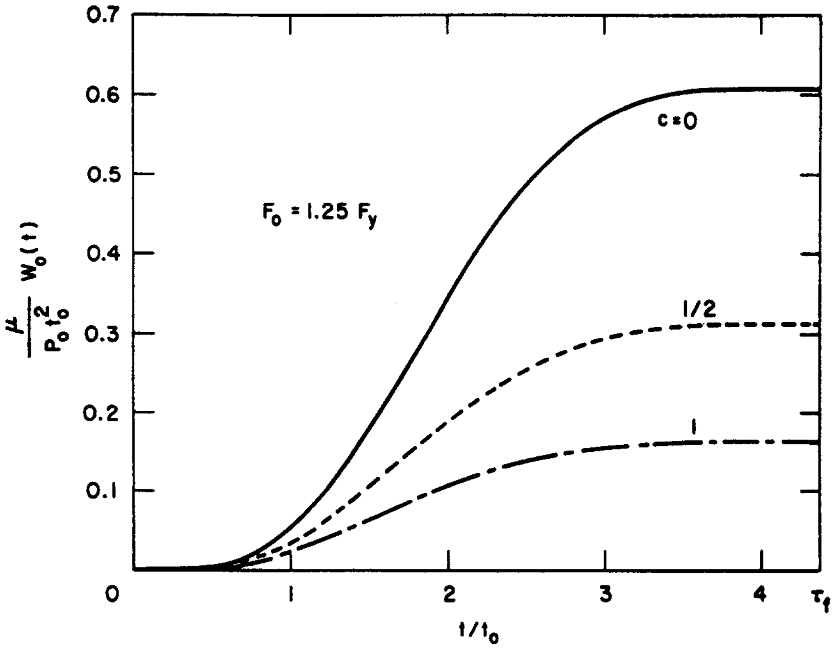

Fig. 9. Deformation history at $r = 0$ for hinge band examples.

These approximate solutions all had the form

$$W_0(t) \approx W^* f(P_e/P_y),$$
$$W^* = CI^2/P_y, \tag{6.2}$$
$$f(P_e/P_y) \to 1 \quad \text{as} \quad P_e/P_y \to \infty,$$

where W^* is the final deformation produced by a pure impulse, and C is a constant depending on the problem geometry and spatial distribution of loading. An arbitrary pulse thus produces essentially the same deformation as a rectangular pulse of magnitude P_e and duration $2t_{mn}$. The form of the function f depends on the pulse shape used to determine it. However, since the forms closely approximate each other, it does not matter which is chosen and the solution for the rectangular pulse is usually the most convenient.

Guided by these previous solutions, we define a mean time and effective force for the infinite plate to be

$$t_{Fm} = \frac{1}{I_{Ff}} \int_{t_y}^{t_f} (t - t_y) F(t) \, dt,$$
$$F_e = I_{Ff}/2t_{Fm}, \tag{6.3}$$

with $F(t)$ and I_{Ff} defined by eqns (3.9) and (5.1). A mean time associated with the moment history $G(t)$ is defined by

$$t_{Gm} = \frac{1}{I_{Gf}} \int_{t_y}^{t_f} (t - t_y) G(t) \, dt, \tag{6.4}$$

and a separability parameter χ is defined by

$$\chi = 1 - t_{Fm}/t_{Gm}. \tag{6.5}$$

We will assume that the solution for the infinite plate can be approximated as

$$W_0(t_f) \approx W^* f(F_e/F_y, \chi), \tag{6.6}$$

with

$$W^* = 3I_{Ff}^4/8\mu F_y I_{Gf}^2 \tag{6.7}$$

as in eqn (5.3).

A. *Separable loading*

Consider a pressure pulse applied over a fixed region R_0 and expressible as in eqns (5.4) as the product of a load shape $\phi(r)$ and a pulse shape $\psi(t)$. Then, for a specific load shape $\phi(r)$, $G(t)$ is proportional to $F(t)$, i.e.

$$G(t) = C_1 F(t), \tag{6.8}$$

with

$$C_1 = \frac{\int_0^{R_0} r^2\phi(r)\,\mathrm{d}r}{\int_0^{R_0} r\phi(r)\,\mathrm{d}r}. \tag{6.9}$$

This implies

$$I_{Gf} = C_1 I_{Ff}, \qquad t_{Gm} = t_{Fm}, \qquad \chi = 0. \tag{6.10}$$

Using the solution for the rectangular pulse given by eqn (5.15) to determine the form of the function f, eqns (6.6) and (6.7) become

$$\begin{aligned} W_0(t_f) &\approx W^*(1-F_y/F_e)^3(1+F_y/F_e), \\ W^* &= 3I_{Ff}^2/8\mu C_1^2 F_y, \end{aligned} \tag{6.11}$$

which are analogous to eqns (6.2).

The approximation given by eqns (6.11) was found to be valid for a wide variety of pulse shapes. In particular, the results shown in Fig. 3 for the loading given by eqns (5.6) are shown again in Fig. 10 as a function of F_e/F_y. The curves for $\frac{1}{4} < b < \infty$ fall between those shown, and the curve for $b = \infty$ coincides with the correlation given by eqns (6.11). The effective force is

$$\begin{aligned} F_e &= \frac{(b+2)F_y^2}{2(b+1)F_y - bF_0} \quad \text{for} \quad \frac{F_0}{F_y} < \frac{b+1}{b}, \\ &= \frac{b(b+2)}{(b+1)^2}F_0 \quad \text{for} \quad \frac{F_0}{F_y} \geqslant \frac{b+1}{b}. \end{aligned} \tag{6.12}$$

B. *Nonseparable loading*

We wish to generalize the approximation given by eqns (6.11) to include loadings which cannot be expressed as the product of functions of position and time, and especially, the subset consisting of loadings applied over a time-dependent region of the plate. Solutions for a variety of loadings with arbitrary parameters were investigated and it was found that χ could be used to characterize the relation between the different time-dependencies of $F(t)$ and $G(t)$. The value of χ is small for physically realistic loadings and is zero for separable loadings.

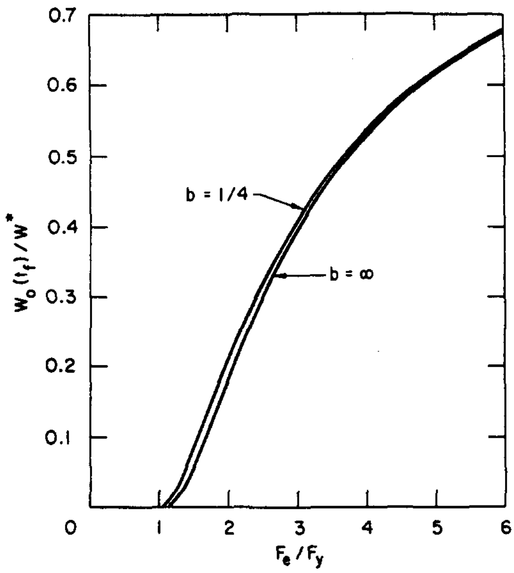

Fig. 10. Final plastic deformation as function of effective force for separable loading example.

Consider loadings of the form

$$P(r,t) = P_0\psi(t)\phi(r/R(t)), \qquad 0 \leqslant r \leqslant R(t), \qquad = 0, \qquad r > R(t), \tag{6.13}$$

with

$$R(0) = R_0, \qquad \psi(0) = 1, \qquad \phi(0) = 1.$$

Then, for $\rho(t) \geqslant R(t)$,

$$F(t) = P_0\psi(t)R^2(t)\phi_F, \qquad G(t) = P_0\psi(t)R^3(t)\phi_G, \tag{6.14}$$

with ϕ_F and ϕ_G defined by

$$\phi_F = \int_0^1 y\phi(y)\,\mathrm{d}y, \qquad \phi_G = \int_0^1 y^2\phi(y)\,\mathrm{d}y. \tag{6.15}$$

More specifically, take

$$R(t) = R_0[1+\beta(t/t_0)^c], \qquad \phi(r/R) = 1-[r/R(t)]^a, \qquad F(t) = F_0[1-(t/t_0)^b], \quad 0 \leqslant t \leqslant t_0, \qquad = 0, \quad t > t_0, \tag{6.16}$$

with

$$a > 0, \qquad b > 0, \qquad c > 0, \qquad \beta \geqslant 0.$$

Using eqn (6.13), $\psi(t)$ is found to be

$$\psi(t) = \frac{[1-(t/t_0)^b]}{[1+\beta(t/t_0)^c]^2}, \qquad 0 \leqslant t \leqslant t_0, \tag{6.17}$$
$$= 0, \qquad t > t_0,$$

and

$$F_0 = P_0 R_0^2 \phi_F. \tag{6.18}$$

The initial decay rate of the applied force $F(t)$ is rapid if b is small and slow if b is large. Similarly, the initial growth of the radius $R(t)$ of the loaded region is rapid if c is small and slow if c is large. The radius grows from R_0 to $R_0(1+\beta)$ in time t_0, and the loading reduces to the case given by eqns (5.6) when $\beta = 0$.

For $F_0/F_y < (b+1)/b$, the motion stops before t_0 and

$$\tau_f = t_f/t_0 = [(b+1)(1-F_y/F_0)]^{1/b},$$
$$F_e = \frac{(b+2)F_y^2}{2(b+1)F_y - bF_0},$$
$$t_{Fm} = t_f \frac{[2(b+1)F_y - bF_0]}{2(b+2)F_y}, \tag{6.19}$$
$$t_{Gm} = t_f \left\{ \frac{\dfrac{2(b+1)F_y - bF_0}{2(b+2)} + \dfrac{\beta\tau_f^c}{(b+c+2)}\left[(b+1)F_y - \dfrac{b(c+1)}{c+2}F_0\right]}{F_y + \dfrac{\beta\tau_f^c}{(b+c+1)}\left[(b+1)F_y - \dfrac{bc}{c+1}F_0\right]} \right\},$$
$$\chi = 1 - t_{Fm}/t_{Gm}.$$

For $F_0/F_y \geqslant (b+1)/b$,

$$\tau_f = [b/(b+1)](F_0/F_y),$$
$$F_e = [b(b+2)/(b+1)^2]F_0, \tag{6.20}$$
$$\chi = \frac{\beta c(b^2+bc+3b+3c+4)}{(c+1)(b+c+1)[(c+2)(b+c+2)+2\beta(b+2)]}.$$

Using eqns (6.20) to eliminate F_0 and β in favor of F_e and χ, the solution for the final plastic deformation at $r = 0$ is, for $F_e/F_y \geqslant (b+2)/(b+1)$,

$$W_0(t_f) = W^*\left[1 + \sum_{n=1}^{4} B_n(b,c,\chi)\left(\frac{F_y}{F_e}\right)^n\right], \tag{6.21}$$

where W^* is defined by eqn (5.3). The B_n coefficients are

$$B_n(b,c,\chi) = \frac{24(-1)^n}{(4-n)!\,n!}\left(\frac{b+2}{b+1}\right)^n\left\{1 - n\left(\frac{b+1}{b}\right)^{2-n}(1-\chi)^2\int_0^1 \frac{\tau[H_1(b,\tau)]^{4-n}\,d\tau}{[H_1(b,\tau)-\chi H_2(b,c,\tau)]^2}\right\}, \tag{6.22}$$

with

$$H_1(b,\tau) = 1 - \tau^b/(b+1),$$
$$H_2(b,c,\tau) = \{2(b+2)(c+1)(b+c+1)H_1(b,\tau) + (c+2)(b+c+2) \tag{6.23}$$
$$\times [bc-(b+1)(c+1)H_1(b,\tau)]\tau^c\}/[c(b^2+bc+3b+3c+4)].$$

The integrals in eqn (6.22) can be evaluated numerically, or after expanding in series in χ, they can be integrated in closed form for some combinations of b and c. For small χ, the results for B_n depend only very weakly on b and c, i.e.

$$B_n(b, c, \chi) \approx \bar{B}_n(\chi). \tag{6.24}$$

Moreover, the B_n are interrelated such that

$$\begin{aligned} B_1(b, c, \chi) &\approx B(\chi) - 3, \\ B_2(b, c, \chi) &\approx 3 - 3B(\chi), \\ B_3(b, c, \chi) &\approx 3B(\chi) - 1, \\ B_4(b, c, \chi) &\approx -B(\chi), \end{aligned} \tag{6.25}$$

and a good fit to the results is given by

$$B(\chi) \approx 1/(1-2\chi)^2. \tag{6.26}$$

Consequently,

$$W_0(t_f) \approx W^*\left(1 - \frac{F_y}{F_e}\right)^3 \left[1 + \frac{F_y}{F_e(1-2\chi)^2}\right], \tag{6.27}$$

which reduces to eqn (6.11) for $\chi = 0$.

The solid curve on Fig. 11 shows $W_0(t_f)/W^*$ for $a = 1$, $b = c = \frac{1}{4}$, and $\beta = 1.875$. This combination of coefficients corresponds to $\chi = 0.1$, and the dashed curve shows the approximation given by eqn (6.27) for this value of χ. Results for larger values of b and c fall between the two curves.

Figure 12 shows β as a function of b for $F_0/F_y \geqslant (b+1)/b$ and $\chi = 0.05$, 0.1 and 0.2; the solid curves are for $c = b$ and the dashed curves are for $c = 1/b$. We note that χ is small for wide ranges of β, b and c. In general, χ is a small quantity for physically plausible loadings.

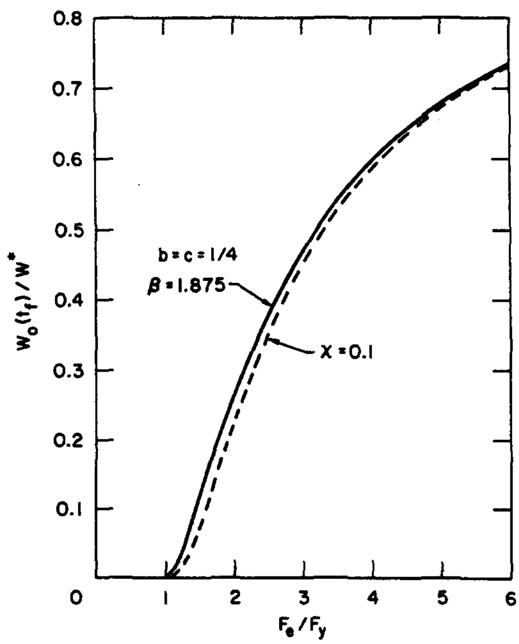

Fig. 11. Final plastic deformation as function of effective force with $\chi = 0.1$ for growing load region.

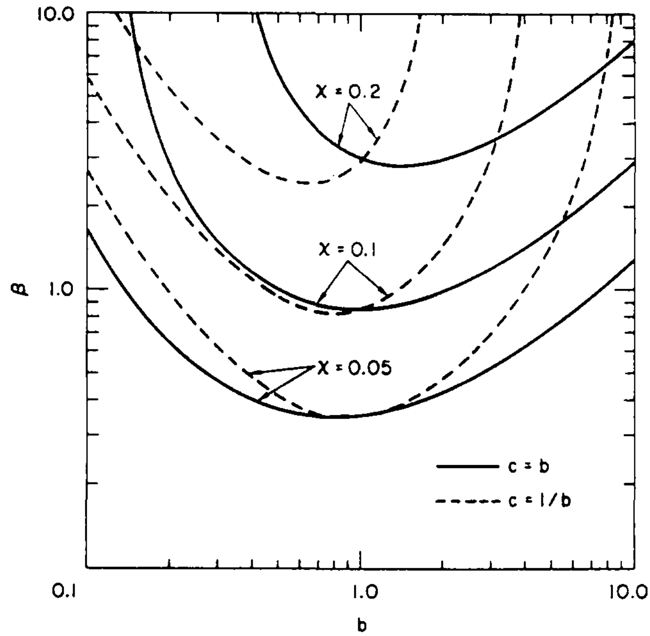

Fig. 12. Relationship between b, c, β and χ for growing load-region example.

The approximation formula was found to be valid for a wide variety of load shapes. In particular, for the hinge band problems prescribed by eqns (5.21)–(5.23), the effective force and the parameter χ as determined from eqns (6.3) and (6.5) are $F_e = 1.47F_0$ and $\chi = 0$, 0.08277 and 0.15098 for $c = 0$, $\frac{1}{2}$ and 1, respectively. Table 1 gives the final central deflection computed from the exact solution and from the approximation of eqn (6.27) for various combinations of c and F_0/F_y.

Equation (6.27) provides a good approximation to the exact solution for problems where the loaded region grows over a finite time interval. The hinge radius $\rho(t)$ may be less than $R(t)$ for a significant interval if the loaded region grows indefinitely; it is then preferable to solve eqn (3.5) iteratively for $\rho(t)$ and evaluate the exact solution.

Acknowledgment—One of us (C.K.Y.) would like to acknowledge the support of the Office of Basic Energy Sciences, U.S. Department of Energy.

Table 1. Comparison of exact and approximate solutions for hinge band problems

		$W_0(t_f)\mu/(P_0t_0^2)$	
c	F_0/F_y	Exact	Approximate
0	1.25	0.6079	0.5597
0	2.5	3.776	3.756
0	5.0	11.223	11.218
1/2	1.25	0.3129	0.3022
1/2	2.5	1.9244	1.9217
1/2	5.0	5.5288	5.5237
1	1.25	0.1631	0.1599
1	2.5	0.9681	0.9590
1	5.0	2.6524	2.6325

REFERENCES

1. P. S. Symonds, Elastic, finite deflection and strain rate effects in a mode approximation technique for plastic deformation of pulse loaded structures. *J. Mech. Engng Sci.* **22,** 189–197 (1980).
2. P. S. Symonds, Finite elastic and plastic deformations of pulse loaded structures by an extended mode technique. *Int. J. Mech. Sci.* **22,** 597–605 (1980).
3. P. S. Symonds and T. Wierzbicki, Membrane mode solutions for impulsively loaded circular plates. *J. Appl. Mech.* **46,** 58–64 (1979).
4. J. B. Martin, The determination of mode shapes for dynamically loaded rigid-plastic structures. *Meccanica* **16,** 42–45 (1981).
5. N. Jones and T. Wierzbicki, A study of the higher modal dynamic plastic response of beams. *Int. J. Mech. Sci.* **18,** 533–542 (1976).
6. C. K. Youngdahl, Correlation parameters for eliminating the effect of pulse shape on dynamic plastic deformation. *J. Appl. Mech.* **37,** 744–752 (1970).
7. D. Krajcinovic, On approximate solutions for rigid-plastic structures subjected to dynamic loading. *Int. J. Non-Linear Mech.* **7,** 571–575 (1972).
8. N. Cristescu, Dynamic plasticity. *Appl. Mech. Rev.* **21,** 659–668 (1968).
9. D. Krajcinovic, Dynamic response of rigid ideally plastic structures. *Shock Vib. Dig.* **5,** 2–9 (1973).
10. N. Jones, A literature review of the dynamic plastic response of structures. *Shock Vib. Dig.* **7,** 89–105 (1975).
11. N. Jones, Recent progress in the dynamic plastic behavior of structures, Part I. *Shock Vib. Dig.* **10,** 21–33 (1978).
12. N. Jones, Recent progress in the dynamic plastic behavior of structures, Part II. *Shock Vib. Dig.* **10,** 13–19 (1978).
13. N. Jones, Recent progress in the dynamic plastic behavior of structures, Part III. *Shock Vib. Dig.* **13,** 3–16 (1981).
14. W. E. Baker, Approximate techniques for plastic deformation of structures under impulsive loading. *Shock Vib. Dig.* **7,** 107–117 (1975).
15. W. Baker, Approximate techniques for plastic deformation of structures under impulsive loading, II. *Shock Vib. Dig.* **11,** 19–24 (1979).
16. P. P. Perzyna, Dynamic load carrying capacity of a circular plate. *Archwm Mech. stosow.* **10,** 635–647 (1958).
17. C. K. Youngdahl, Influence of pulse shape on the final plastic deformation of a circular plate. *Int. J. Solids Struct.* **7,** 1127–1142 (1971).
18. M. F. Conroy, Rigid-plastic analysis of a simply-supported circular plate due to dynamic circular loading. *J. Franklin Inst.* **288,** 121–135 (1969).
19. A. L. Florence, Clamped circular rigid-plastic plates under central blast loading. *Int. J. Solids Struct.* **2,** 319–335 (1966).
20. D. Krajcinovic, Clamped circular rigid-plastic plates subjected to central blast loading. *Comput. Struct.* **2,** 487–496 (1972).
21. A. L. Florence, Response of circular plates to central pulse loading. *Int. J. Solids Struct.* **13,** 1091–1102 (1977).
22. Yu. R. Lepik, On the dynamical flexure of infinite plastic-rigid plates. *Sov. Appl. Mech.* **10,** 615–619 (1974).